Objective Estimates of the Seismic Intensity of the 1755 Lisbon Earthquake

D. R. BRILLINGER[1], AND [B. A. BOLT[2]]

[1]*Statistics, University of California, Berkeley*
[2]*Geology and Geophysics, University of California, Berkeley*

Dedicated to Bruce Bolt, my friend, colleague and collaborator.

ABSTRACT

A probabilistic method that takes account of the ordinal character of the MSK Scale has been adapted to generate a 1755 seismic intensity map for the Iberian Peninsula. Statistical models are employed to estimate isoseismals and to compute standard error uncertainties. The output includes intensity maps, estimates of the effects associated with each intensity level, and estimates of the distribution of intensity levels a given distance from the hypercenter. It is applied to a data set of Portugese and Spanish intensity values. It is shown how the analysis may be employed to include explanatory variables such as regional and local geological effects.

INTRODUCTION

Substantial tragic effects result from great earthquakes – damage, deaths, tsunamis. Various groups, including seismologists, seismic engineers, government officials and insurers seek to quantify the effects in order to proceed with their work. The quantification methods employed include seismic intensity scales and damageability matrices particularly. Principal intensity scales employed are: the Modified Mercalli, the MSK, and the European Macroseismic Scale. The scale values are typically denoted by roman numerals to reflect the fact that they are derived via verbal descriptions rather than some numerical physical measuring device.

Intensity scales are ordinal, that is the levels are qualitative ordered, the level spacing does not matter, and adjacent categories can be merged. One is not meant to employ the values using the rules of ordinary arithmetic. One purpose of this research is to examine the possibility of assessing formally if the data may be employed as if numerical-valued. A probability approach is adopted and there are advantages. These include: one can examine scientific hypotheses formally, one can assess goodness of fit, one can compute and show uncertainty, one can compare alternate models, and there are often robust/resistant variants of general techniques. The broadly ranging subject matter of statistics becomes available.

Isoseismals are often on a map to indicate seismic intensity experienced. These isoseismals are meant to be contours of equal intensity, to bound areas within which the predominant intensity is the same. The lines prove useful to quantify the shaking pattern and to understand the damage. Traditionally isoseismal maps had been prepared by hand-drawing curves encompassing the observed intensities. The artist seeks to draw a curve encircling, say all the VIII value locations, ignoring scattered VIIIs. Professor Bolt once emphasized to this writer, [Brillinger, 1993], that a critical aspect of existing isoseismal maps, namely that they are conservative in two senses. First, the indicated intensity level at a location is the highest noted. Second, the isoseismals themselves are drawn as far out from the source as reasonable to include all locations with given intensity. However as [Reiter, 1990] states, "… *drawing isoseismals can be a subjective process that may lead to different outcomes for different analyses.*" and this provides a motivation for the present work.

[Perkins and Boatwright,1995] list some of the factors on which seismic intensities depend, namely, size of the earthquake, distance of the site from the earthquake source, the focusing of the earthquake energy and the regional and local geological effects. There is a falloff in severity of effect with distance from the source and substantial variability is inevitably present.

The event of concern is the Lisbon 1 November 1755 tragedy. General descriptions of the event can be found abound. Its magnitude has been estimated as 8.7, depth 20-40km and epicentre at (-10.0,36.5) a point about 90km SW of Sagres. The data employed in the work were provided by J. M. Miranda, who acknowledged Mezcua. There are 810 observations in Portugal and Spain. The counts of the numbers of the various MSK intensities recorded are provided in Table 1 at the end of the paper. There are intermediate levels in the data set but because such are not part of the MSK scale they are not included in the analyses presented.

Figure 1, also at the end of the paper, shows the locations of the measurements for the integral intensities. The clusters are associated with population centers. One sees a falloff from level X to level II as one moves north and east from Sagres.

Other references using intensity values to understand this event include: [Mendes-Victor et al., 1999], [Baptista et al, 2003], [Matrinez Solares, Lopez Arroyo, 2004].

There is discussion of seismic damage scales in [Bullen and Bolt, 1985, pp. 433-437], and [Reiter, 1990].

OBJECTIVES

A prime objective of the work is to further develop an automatic way to prepare isoseismal type maps, a method taking specific note of the ordinal character of the intensity scale data. A second is to provide a probabilistic model, for the circumstance, which can be employed in probabilistic risk assessments. Related work was carried out for the 1989 Loma Prieta event in [Brillinger,1993], [Brillinger,1997], and [Brillinger et al.,2001], and for the 1994 Northridge event in [Brillinger,2003]. Other researchers' papers include: [De Rubeis et al, 1992], [Pettenati et al, 1999], [Wald et al, 1999].

METHODS

Statistical methods have proven useful in addressing problems of insurance, risk management and seismic engineering, in particular techniques based on random process concepts. These include the point process for locations,

$$Y(x,y) = \sum_j \delta(x-x_j,y-y_j)$$

with δ the Dirac delta function and the marked point process

$$Y(x,y) = \sum_j M_j\delta(x-x_j,y-y_j)$$

with the marks, M_j , providing a measure of the severity of the event. In the present case the mark values are {II, III, IV, …, X}. Both specific and general models have been developed for point and marked point processes. These processes are basic to probabilistic seismic risk assessment, [Ogata, 1983] and Vere-Jones, 1992]

For ordinal data the grouped continuous model, [McCullagh and Nelder,1989] is effective. It involves, a latent (or state) random variable, ζ and cutpoints θ_j. The leading to representing intensity data values, Y, as

$$Y=II \text{ if } \zeta < \theta_{II}$$

$$= j \text{ if } \theta_{j-1} <\zeta < \theta_j \text{ if } j = II, III, \dots, IX$$

$$= X \text{ if } \theta_{IX} <\zeta$$

The θ_j are to be increasing.

A strength of the model is that an explanatory X may be introduced directly by setting

$$\zeta = -\beta'X+\varepsilon$$

with β a coefficient to be determined from the data.

If one assumes that ε has an extreme value distribution, then

$$\text{Prob}\{Y=j|X\} = \exp\{-\exp\{ \theta_{j-1}+\beta'X\}-\exp\{-\exp\{\theta_j+\beta'X\}\} \quad (1)$$

The use of an extreme value distribution may be motivated by the character of the situation. Its reasonableness may be checked empirically. For this model the β's and the θ's may be obtained using functions in standard statistical programs. To do so one writes the joint probability as

$$\text{Prob}\{Y=II\}\ \text{Prob}\{Y=III|Y>II\} \dots \text{Prob}\{Y=j|Y>j-1\}$$

An estimate of $E\{\zeta|X\}$ is then provided by

$$-b'X + \gamma$$

where b is the estimate of β and γ is Euler's constant.

In the spatial case at hand one takes

$$\beta'X = \beta(x,y)$$

with j intensity, x longitude and y latitude. In the analyses it will be assumed that β is smooth and that $\varepsilon=\varepsilon(x,y)$ white noise.

From (1)

$$\text{Prob}\{Y(x,y)\le j|X\} = 1 - \exp\{-\exp\{ \theta_j+\beta(x,y)\}\}$$

In summary the model is

$$\text{Prob}\{Y(x,y)=j|X\} = \pi_j(x,y)$$

with $\pi_j(x,y)$ of parametric form and given by (1) above.

Spatial dependence may be introduced through assumptions on the process $\{\varepsilon(x,y)\}$.

RESULTS

Table 1 below gives the counts of numbers of occurrences of the various MSK values in the data set employed. Figure 2 provides a histogram of the data values. One notices a lack of intensity+ values in some cases, for this reason, and because the official MSK scale is integer-valued only the integer-valued intensities are employed in the computations of the paper.

FIGURE 2: Histogram of intensity values in data set

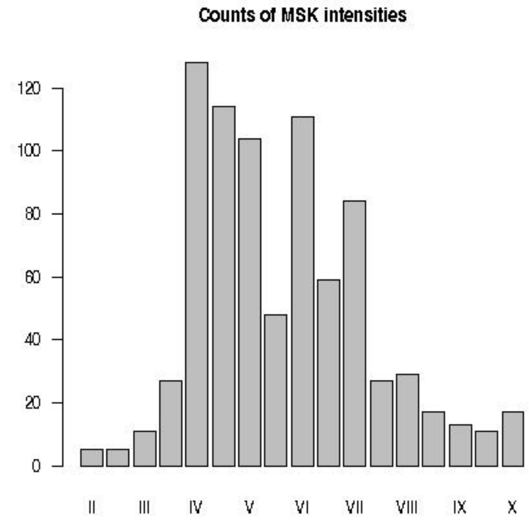

As indicated above Figure 1 provides the locations and intensities of the data employed. The estimated epicenter is indicated in the figure by a * . It is located in the lower left corner and its coordinates have been taken from [Martinez-Solares, Lopez-Arroyo, 2004].

Figures 3 and 4 present the results of fitting the grouped continuous model with the distribution (1). Figure 3 is the estimate of the linear predictor component $\beta(x,y)$. Its interpretation is as a background representing a smooth regional effect, in the presence of the intensity terms. The breakpoints for the color scale have been taken as uniformly spaced across the range of values of the estimate. One sees it to be approximately constant across the region.

FIGURE 3: Estimated β

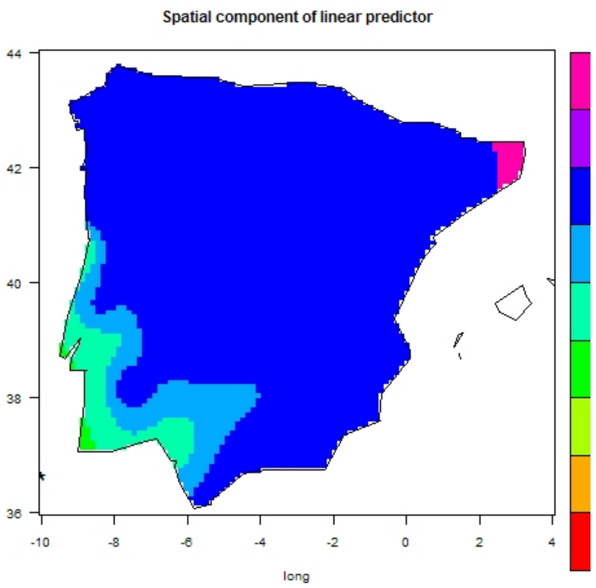

Figure 4 provides the estimates of the θ_j and ±2 s.e. limits. The estimates are seen to be increasing steadily, approximately linearly. This gives some credance to the treatment of the intensity scale as interval. The rightmost cutpoint estimate is seen to be highly variable. This may result from the tangle of IX and X intensities in the lower left corner.

FIGURE 4: Estimated θ_i

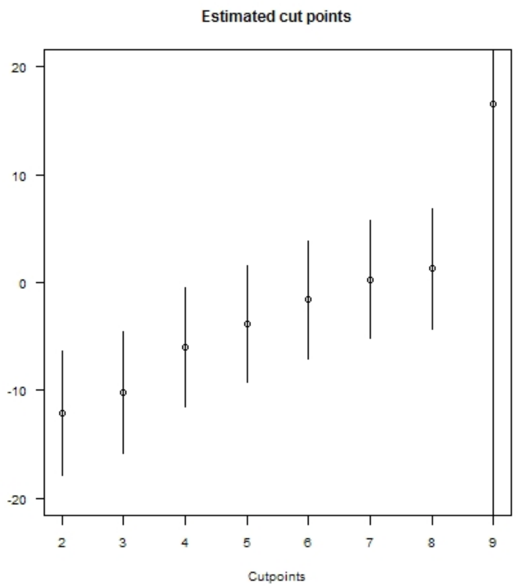

FIGURE 5: Empirical Probabilities

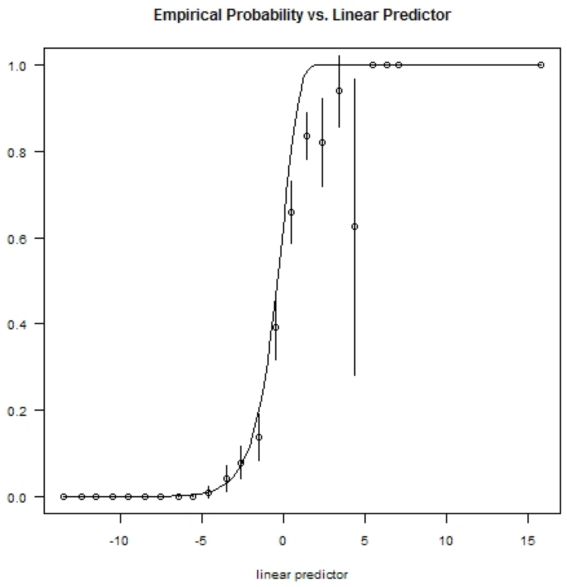

Figure 5 provides the results of a procedure used to assess the fit of the model (1). One plots the proportion of 1's in a given cell of linear predictor values versus the cell midpoint. The continuous curve is the cumulative distribution function of the extreme value distribution. Also ±2 standard error limits have been added to the proportions. There is a suggestion that perhaps another distribution would do better, or perhaps that other explanatories need to be included in the model.

For a given location one can now estimate the probabilities of the various MSK intensities occurring. Figures 6, 7 and 8 provide estimates for intensities X, VII and II respectively.

FIGURE 6: Estimated probabilities for MSK X

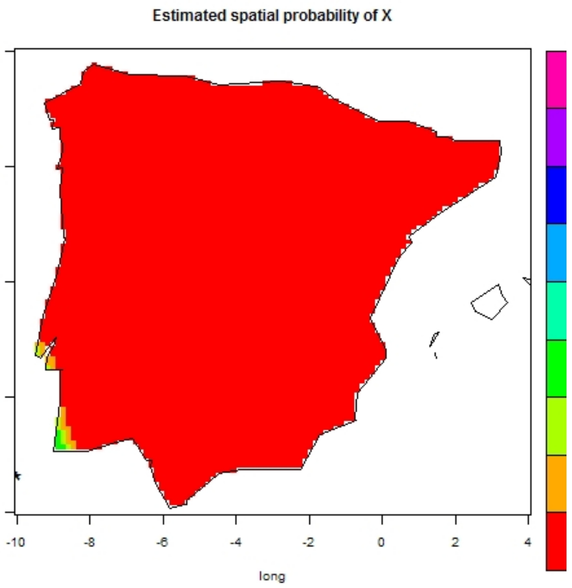

The color scale for the probabilities has been taken to be equispaced from 0 to 1. Unsurprisingly the X-probability is noteable only in the southwest corner of the figure.

Next is the figure for intensity VII.

FIGURE 7: Estimated probabilities for intensity VII.

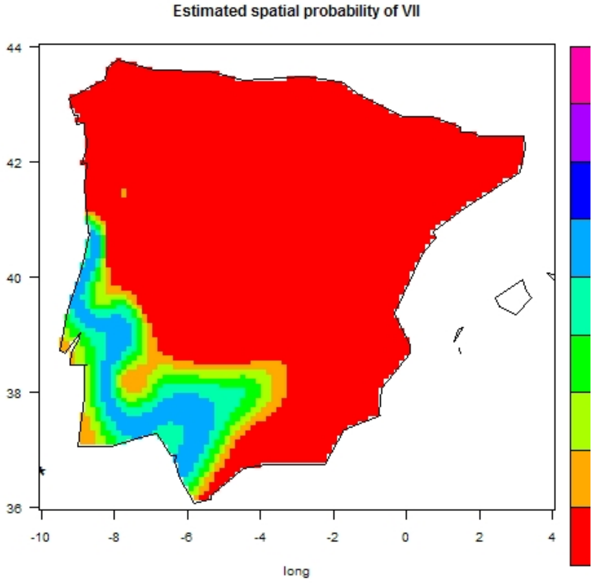

One sees the probabilities are elevated in a strip near the southeast corner. This fits with the distribution of intensity values seen in Figure 1.

Lastly in Figure 8 an estimate of Prob{Y = II | (x,y)} is plotted for the case of intensity II. The values are near 1 in the northeast corner.

FIGURE 8: Estimated probabilities for intensity II

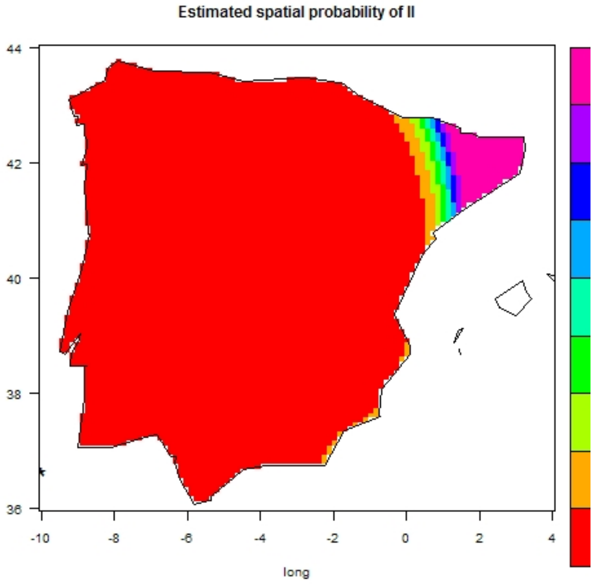

Now there is a (fitted) distribution of intensities for each pixel. This can be used to estimate various risks and other quantities.

Consider next how the intensity falls off with distance of a location from the hypercenter of the event. Figure 9 is a scatter plot of intensity against the logarithm of the distance. One sees a general falloff with lots of scatter.

FIGURE 9: Intensity values versus distance from source

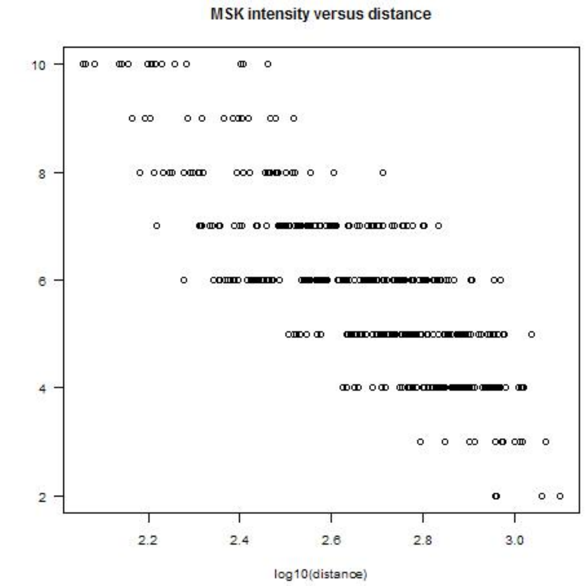

It is convenient, for certain types of computations, to have a specific functional form for the falloff of intensity with distance. Following [Joyner and Boore, 1981] the form

$$\log(-\log(1-\text{Prob}\{Y=j\})) = \alpha_j + \beta d + \gamma \log(d)$$

was employed in [Brillinger, 1996], [Brillinger, 2003] for the ordinal-valued intensity case. Figure 10 shows fitted curves for the cases of intensities X, VII, and II.

FIGURE 10: Joyner-Boore type curve fits to intensity falloff

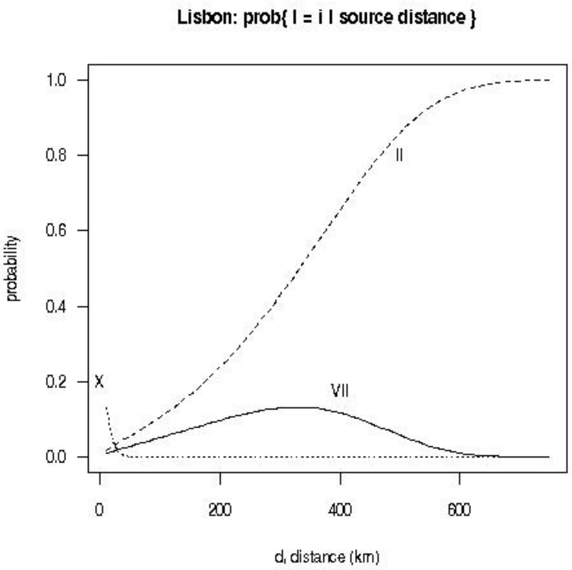

The intensity X probabilities are only noticeable at short distances. The intensity VII probabilities peak around 350km and the intensity II curve quickly rises towards 1.

DISCUSSION AND CONCLUSIONS

In the end the research has not produced isoseismal values, rather it has produced empirical relations and images for the probabilities of various intensities as functions of location or distance. The former appear the more useful entity for feeding into computations and estimations, such as of loss ratios, occurring in later stages of risk analyses.

The study of course has limitations. The methods were based on assumed models, which may not hold. The extreme value distribution had particular computational convenience, but others may prove useful. The methods involved tuning parameters, which need to be chosen.

The greatest limitation is perhaps not including other explanatory variables in the models. For example it was hoped to have site conditions to include in the model/analysis. Doing so is not complicated for they could be introduced into the explanatory variable X directly. (This was one of the things that Professor Bolt was working on incorporating into the study.)

ACKNOWLEDGEMENTS

Bruce Bolt introduced me to so many of the important concepts of seismology and earthquake engineering. It is hard to find words of gratitude for his having shared so much knowledge with me. This paper would have been surely much better had he been available to contribute more.

Bob Wiegel, another Berkeley colleague, helped me to understand some of the research concerned with locating the source of the earthquake. J. M. Martinez-Solares, and J. M. Miranda provided the intensity data employed in the study. I thank them also.

The research was supported by the NSF grants DMS-20010831 and DMS-20051127.

REFERENCES

Baptista, M. A., Miranda, J. M., Chierici, F., Zitellini. New study of the 1755 earthquale source based on multi-channel seismic survey data and tsunami modelling. Natural Hazards and earth System Science 3. pp. 333-340.

Brillinger, D. R. Earthquake risk and insurance, Environmetrics 4, pp. 1-21. 1993.

Brillinger, D. R. Random process methods and environmental data: the 1996 Hunter Lecture, Environmetrics 8, pp. 269-281. 1997.

Brillinger, D. R. Three environmental probabilistic risk problems, Statistical Science 18, pp. 412-421. 2003

Brillinger, D. R., Chiann, C., Irizarry, R. A., Morettin, P. A. Automatic methods for generating seismic intensity maps., J. Applied Probability 38A, pp. 188-201. 2001.

Bullen, K. E. , Bolt, B. A. An Introduction to the Theory of Seismology, Fourth Edition. Cambridge U. Press, Cambridge. 1985.

De Rubeis, V., Gasparini, C., Maramai, I., Murru, M., Tertulani, A. The uncertainty and ambiguity of isoseismal maps. Earthquake Engineering Structural Dynamics 21, pp. 509-523. 1992.

Joyner, W.B., Boore, D. M. Peak horizontal acceleration and velocity from strong motion records from 1979 Imperial Valley, California. Bulletin Seismological Society of America 71, pp. 2011-2038.

Marrtinez-Solares, J. M., Lopez-Arroyo, A. The great historical 1755 earthquake, effects and damages in Spain, J. Seismology 8, pp 275-294. 2004.

McCullagh, P. Nelder, J. A. Generalized Linear Models, Second Edition. Chapman and Hall, New York. 1989.

Mendes-Victor, L., Baptista, M. A., Miranda, J. M., Miranda, P. M., Can Hydrodynamic Modelling of Tsunami Contribute to Seismic Risk Assessment? Phys. Chem. Earth 24, pp. 139-144. 1999.

Ogata, Y. Likelihood analysis of point processes and its application to seismological problems. Bulletin International Statistical Institute 50, 943-961.

Perkins, J. B. and Boatwright, J. On Shaky Ground. ABAG, Oakland. 1995.

Pettenati, F., Sirovich, L., and Cavallini, F. Objective treatment and synthesis of macroseismic intensity data sets using tessellation. Bulletin Seismological Society of America 98, pp. 1203-1213. 1999.

Reiter, L. Earthquake Hazard Analysis. Columbia, New York. 1990.

Vere-Jones, D. Statistical methods for the description and display of earthquake catalogs. Statistics and Environmental Sciences (ed. A. T. Walden and P. Guttorp) Halstead, New York, pp. 220-246. 1992.

Wald, D., Quitoriano, V., Dengler, L. A., and Dewey, J. W. Utilization of the internet for rapid community intensity maps. Seismology Research Letters 70, pp. 680-697. 1999

TABLE 1: Observed MSK intensities and counts

II	II+	III	III+	IV	IV+	V	V+	VI	VI+	VII	VII+	VIII	VIII+	IX	IX+	X
5	5	11	27	128	114	104	48	111	59	84	27	29	17	13	11	17

FIGURE 1: Locations and intensity values